Search for $Z\gamma$ high-mass resonances using the ATLAS detector

G Mokgatitswane[1], S Dahbi[1], N P Rapheeha[1], B Mellado[1,2] and X Ruan[1]

[1] School of Physics and Institute for Collider Particle Physics, University of the Witwatersrand, Johannesburg, Wits 2050, South Africa
[2] iThemba LABS, North, Empire Road, Braamfontein 2000, Johannesburg

E-mail: gaogalalwe.mokgatitswane@cern.ch

Abstract. This study presents a search for high-mass resonances in the $Z\gamma$ final states. The search is performed using the Monte Carlo simulated signal samples of mass from 200 GeV up to 5 TeV, corresponding to an integrated luminosity of 139 fb^{-1} dataset recorded by the ATLAS experiment in proton-proton collisions during the LHC Run 2. Only the leptonic decay of the Z boson to a lepton-antilepton pair $\mu^+\mu^-$ is considered. The analysis search for a localized excess in the invariant mass distribution of reconstructed final state over a smoothly-falling background emanating from Standard Model processes. The characterization of signal shape for the mass spectrum from gluon fusion production mode is modelled by a double-sided crystal ball function form and the background shape modelling is performed using analytic functions of different orders. The systematic uncertainties are incorporated, which arise from several experimantal sources and on the possible bias (spurious signal) on the fitted signal yield due to the choice of background function.

1. Introduction

The discovery of new boson consistent with the Standard Model (SM) Higgs Boson h by the ATLAS and CMS experiments [1,2] at the Large Hadron Collider (LHC) opened a wide range of research focus to studying the nature of the Higgs boson and allows to investigate a wide scope of physical phenomena. This includes theoretical modelling of Higgs boson production processes and searches for physics Beyond the Standard Model (BSM) which might be discovered with large dataset from the LHC.

A 2HDM+S model, where S is a singlet scalar, was used in Ref. [3,4] to explain some features of the Run 1 LHC data. Here the heavy scalar, H, decays predominantly into SS, Sh, where h is the SM Higgs boson. The model predicts the emergence of multi-lepton anomalies that have been verified in Refs. [5–8], where a possible candidate of S has been reported in Ref. [9]. The model can further elaborate on multiple anomalies in astro-physics if it is complemented by a candidate of a Dark matter [10]. It can be easily extended [11] to account for the muon $g-2$ anomaly (see Ref. [12] for a review of anomalies). This further motivates searches for heavy resonances decaying into $Z\gamma$.

The study aims at developing a search for high-mass $Z\gamma$ resonances of mass from 200 GeV up to 5 TeV. Here we consider a hypothetical heavy scalar H decaying to $Z\gamma$ ($H \to Z\gamma$) as shown in Fig. 1, where only events in which the Z boson decays to di-electrons or di-muons are used. The

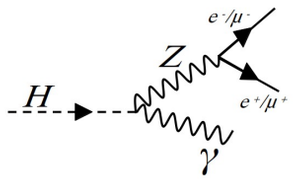

Figure 1: A schematic Feynman diagram of the decay of a heavy scalar H.

$Z\gamma$ channel is considered because a Higgs like boson (H) can have relatively higher possibility of decaying into a $Z\gamma$ final state in comparisons with the di-photon final state. In addition, its vertex is well reconstructed than di-photon events, hence making it possible to search for excesses.

However, the resonances which are searched for can not be easily extracted since they are overlayed by background processes with simillar signatures. These backgrounds originate from non-resonant $Z\gamma$ events, either from initial state radiation (diboson production in the t, u channels), from final-state-radiation in radiative Z boson decays ($Z \to \ell\ell\gamma$) or from parton-to-photon fragmentation. Furthermore, the production of a Z boson in association with jets, followed by a $Z \to \ell\ell$ decay and misidentification of a jet as a photon also form part of the background. For other backgrounds, the contribution from $t\bar{t}$ and W/Z are expected to be much smaller and thus they are neglected.

For this study, it is therefore imperative to understand well, the yield of both signal and background events. In order to achieve this, the signal and background modelling is performed using the Double Sided Crystal Ball function (DSCB) and analytic functional forms of a different order, respectively. Systematic uncertainties are also included to account for possible residual mismodelling effects. The study is focusing on the di-muon channel as the first part of the actual full analysis.

2. Signal and Background samples

The Monte Carlo (MC) samples of $Z \to \mu^+\mu^-$ used in this analysis correspond to 2015-18 data condition. These samples are generated using a next-to-leading order (NLO) MC generator POWHEG [13] interfaced to the PYTHIA8 parton shower model [14], with the CT10 parton distribution functions (PDFs) in the matrix element [15]. The AZNLO set of tuned parameters [16] was used in conjunction with CTEQ6L1 PDF set [17] for modelling of non-perturbative effects. The background samples are generated from full simulated $Z\gamma$ with SHERPA [18,19], and Z+jet events obtained through data-driven method by reversing one photon (2D-sideband method) [20].

2.1. Event selection

For this analysis we select photon and muon candidates [18, 21]. The preselected photons are required to have transverse momentum above 15 GeV and those reconstructed within regions of the calorimeter affected by read-out or high-voltage failures are rejected (loose identification requirement). After preselection of photons, the following strigent selections are required:

- Isolation from hadronic activity using "FixedCutLoose" working point. It is based on the energy in a cone and defined as: $E_{\mathrm{T}}^{iso}|_{\Delta R=0.2} < 0.065 \times p_{\mathrm{T}}$ GeV (calorimeter isolation) and $p_{\mathrm{T}}^{iso}|_{R_{max}=0.2} < 0.05 \times p_{\mathrm{T}}$ GeV (track isolation).
- The relative photon p_{T} over $m_{\ell\ell\gamma}$ is required to be over 0.27 GeV.

The di-lepton mass is required to be $76.18 < m_{\ell\ell} < 106.18$ GeV.

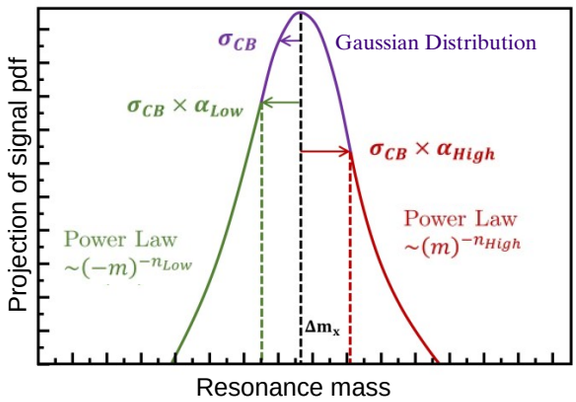

Figure 2: The Double-Sided Crystal Ball function definition.

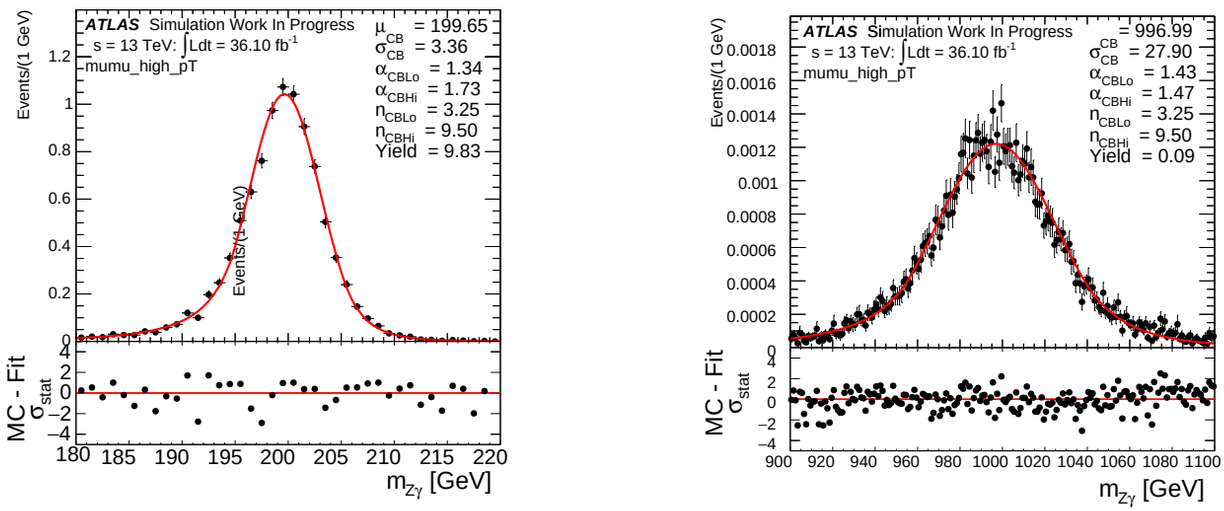

Figure 3: Results of individual fit of DSCB parameters.

3. Signal parameterisation

Characterisation of the $Z\gamma$ invariant mass distribution for high mass resonances is found to be well modelled with a Double-Sided Crystal Ball function (DSCB). The shape and parameters definition of DSCB are shown in Fig. 2.

The DCSB function consists of a core Gaussian with power-law tails on both sides of the mode of the distribution. It is defined as:

$$N. \begin{cases} e^{-t^2/2}, & if \ -\alpha_{Lo} \leq t \leq \alpha_{Hi} \\ \frac{e^{0.5\alpha_{Lo}^2}}{[\frac{\alpha_{Lo}}{n_{Lo}}(\frac{\alpha_{Lo}}{n_{Lo}} - \alpha_{Lo} - t)]^{n_{Lo}}}, & if \ t < -\alpha_{Lo} \\ \frac{e^{0.5\alpha_{Hi}^2}}{[\frac{\alpha_{Hi}}{n_{Hi}}(\frac{\alpha_{Hi}}{n_{Hi}} - \alpha_{Hi} + t)]^{n_{Hi}}}, & if \ t > -\alpha_{Hi}, \end{cases} \quad (1)$$

where $t = \Delta m_x/\sigma_{CB}$, $\Delta m_x = m_x - \mu_{CB}$, N is the normalisation parameter, μ_{CB} is the peak of the Gaussian distribution, σ_{CB} represents the width of Gaussian part of the function, while $\alpha_{Lo}(\alpha_{Hi})$ is the point where the Gaussian becomes a power-law on low (high) mass side and $n_{Lo}(n_{Hi})$ is the exponent of the power-law. The results of the DSCB fits are shown in Fig. 3 for signal mass points $m_X = 200\,\text{GeV}$ and $1000\,\text{GeV}$.

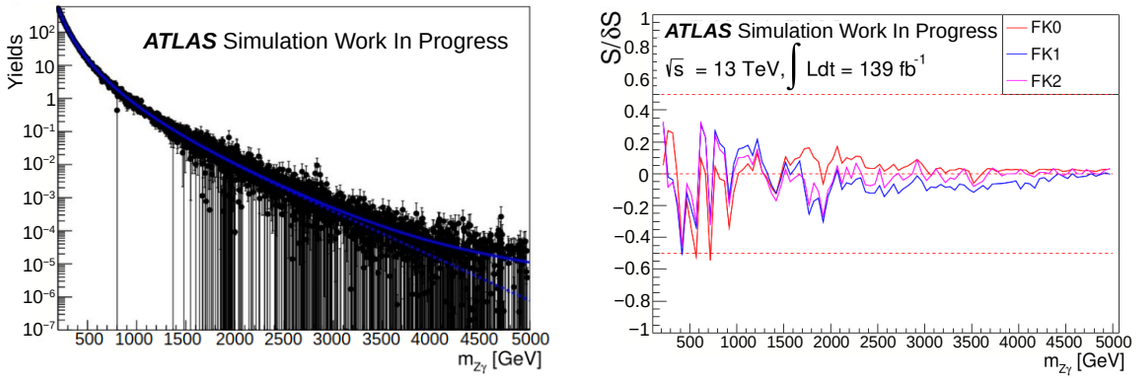

Figure 4: Fitting on the background template [200,5000] GeV with S+B function (left) and Ratio of the fitted spurious signal yield to its uncertainty for the background models as a function of mass for each functional form (right).

4. Background modelling

To estimate the background functional shape, a background template is required which consists of the $Z\gamma$ and Z+jet processes [22]. The template is prepared by combining the background using MC normalised to 90% of data in the signal region ($Z\gamma$ events) and 10% of reverse photon identification data in the control region (Z+jet events) [20]. Here we use the template to find the suitable function to describe background in the data, which gives a small bias on the signal yield (spurious signal) compared to the expected uncertainty from the background fluctuations. The bias over its uncertainity ($S/\delta S$) is expected to be less than 50%.

4.1. Spurious signal

The spurious signal, caused by the choice of a particular background parameterisation is evaluated by fitting a high statistics background sample (template) with a signal plus background model [22]. A scan (20 GeV step) of the existence of fake signal is performed across the m_X window (200 GeV-5000 GeV). Functional forms of different order, of up to third order exponential polynominal are used for modelling:

$$f_k(x;b,a_k) = (1-x)^b x^{\Sigma_{j=0}^{k} a_j log(x)^j}, \tag{2}$$

where $x = \frac{m_{\ell\ell\gamma}}{\sqrt{s}}$, $k = 0, 1, 2$ noted as FK0, FK1 and FK2, respectively, and the b parameter is usually set either to 1/3. Figure 4 (left) shows a mass spectrum of a three-body invariant mass distribution ($m_{\ell\ell\gamma}$), of up to 5000 GeV fitted with signal plus background model. Figure 4 (right) shows the maximum ratio of fitted spurious signal yield to its uncertainty.

5. Systematic uncertainty

5.1. Systematic uncertainty on the signal $m_{\ell\ell\gamma}$ distribution

The systematic uncertainties due to the modelling of the signal invariant mass distribution, have been estimated. For the invariant mass of $Z\gamma$ system, the main sources of systematic uncertainties on signal modelling are e/γ resolution, e/γ energy scale, muon momentum scale or resolution variations.

For the simulated signal MC samples used in this study, the $m_{\ell\ell\gamma}$ distribution is recomputed after varying the former uncertainty sources by $\pm 1\sigma$, where σ is its uncertainty provided by the Muon Combined Performance Working Group (MCP). Systematic uncertainties on the mass position and mass resolution are summarized in Tables 1 and 2, respectively.

Table 1: Summary of systematic uncertainty on signal position (μ_{CB}).

Source	Uncertainty on *Signal position* (%)
e/γ energy scale (all)	(0.38,-0.38)
Muon sagitta resolution bias	(0.00, 0.00)
Muon sagitta angle (ρ)	(0.00, 0.00)
Muon scale	(-0.05,0.05)

Table 2: Summary of systematic uncertainty on signal resolution (σ_{CB}).

Source	Uncertainty on *Signal resolution* (%)
e/γ energy resolution (all)	(2.06,-1.43)
Muon inner detector	(3.35,-2.89)
Muon spectrometer	(2.25,-3.86)

5.2. Systematic uncertainty on the signal efficiency

Table 3 summarizes the systematic uncertainty on the signal efficiency, which is estimated by varying the trigger, reconstruction, isolation and identification scale factors of the leptons by $\pm 1\sigma$. The dominant uncertainty is from muon reconstruction efficiency. There is p_{T}-dependent systematic taking into account the extrapolation of the Z efficiency measurements towards very high p_{T}. According to the MCP, the increase in uncertainty may well be compatible with expectations, depending on the campaign and the kinematics of the events looked at. However, this is not considered a limiting factor for the analysis.

Table 3: Summary of systematic uncertainty on signal efficiencies for $\mu\mu$ channel.

Source	Uncertainty on *Signal efficiency* (%)
Muon isolation efficiency (stat.)	(0.59, -0.59)
Muon isolation efficiency (sys.)	(0.45,-0.39)
Muon reconstruction efficiency (stat.)	(0.13, -0.13)
Muon reconstruction efficiency (sys.)	(15.86,-15.76)
Muon reconstruction efficiency (stat. lowpt)	(0.03,-0.04)
Muon reconstruction efficiency (sys. lowpt)	(0.05, -0.05)
Muon efficiency (ttva stat.)	(0.14, -0.13)
Muon efficiency (ttva sys.)	(0.15, -0.14)
Muon efficiency (trig. stat. uncertainty)	(0.00, 0.00)
Muon efficiency (trig. sys. uncertainty)	(0.00, 0.00)
Photon ID efficiency uncertainty	(0.75, -0.75)
Photon isolation efficiency uncertainty	(1.33, -1.33)
Photon trigger efficiency uncertainty	(0.00, 0.00)
Pile-up	(0.99, -1.76)

6. Conclusion

The aim of this study was to search for high-mass $Z\gamma$ resonances in 200-5000 GeV mass range, using the Monte Carlo simulated signal samples corresponding to an integrated luminosity of $139\,\mathrm{fb}^{-1}$ dataset recorded by the ATLAS experiment in proton-proton collisions during the LHC Run 2. The signal and background modelling have been performed using Double Sided Crystal Ball function and functional forms of up to third order exponential polynominal, respectively. The systematic uncertainties which arise from several experimental sources have been estimated as well as on the possible bias (spurious signal) on the fitted signal yield due to the choice of background function. The analysis is ongoing and aiming at setting up the statistical interpretation.

References

[1] Aad G *et al.* (ATLAS) 2012 *Phys. Lett. B* **716** 1–29 (*Preprint* 1207.7214)
[2] Khachatryan V *et al.* 2017 *Journal of High Energy Physics* **2017** 076
[3] von Buddenbrock S, Chakrabarty N, Cornell A S, Kar D, Kumar M, Mandal T, Mellado B, Mukhopadhyaya B and Reed R G 2015 (*Preprint* 1506.00612)
[4] von Buddenbrock S, Chakrabarty N, Cornell A S, Kar D, Kumar M, Mandal T, Mellado B, Mukhopadhyaya B, Reed R G and Ruan X 2016 *Eur. Phys. J. C* **76** 580 (*Preprint* 1606.01674)
[5] von Buddenbrock S, Cornell A S, Fadol A, Kumar M, Mellado B and Ruan X 2018 *J. Phys. G* **45** 115003 (*Preprint* 1711.07874)
[6] Buddenbrock S, Cornell A S, Fang Y, Fadol Mohammed A, Kumar M, Mellado B and Tomiwa K G 2019 *JHEP* **10** 157 (*Preprint* 1901.05300)
[7] von Buddenbrock S, Ruiz R and Mellado B 2020 *Phys. Lett. B* **811** 135964 (*Preprint* 2009.00032)
[8] Hernandez Y, Kumar M, Cornell A S, Dahbi S E, Fang Y, Lieberman B, Mellado B, Monnakgotla K, Ruan X and Xin S 2021 *Eur. Phys. J. C* **81** 365 (*Preprint* 1912.00699)
[9] Crivellin A, Fang Y, Fischer O, Kumar A, Kumar M, Malwa E, Mellado B, Rapheeha N, Ruan X and Sha Q 2021 (*Preprint* 2109.02650)
[10] Beck G, Kumar M, Malwa E, Mellado B and Temo R 2021 (*Preprint* 2102.10596)
[11] Sabatta D, Cornell A S, Goyal A, Kumar M, Mellado B and Ruan X 2020 *Chin. Phys. C* **44** 063103 (*Preprint* 1909.03969)
[12] Fischer O *et al.* 2021 *Unveiling hidden Physics Beyond the Standard Model at the LHC* (*Preprint* 2109.06065)
[13] Alioli S, Nason P, Oleari C and Re E 2008 *Journal of High Energy Physics* **2008** 060–060
[14] Sjöstrand T, Mrenna S and Skands P 2008 *Computer Physics Communications* **178** 852–867
[15] Lai H L, Guzzi M, Huston J, Li Z, Nadolsky P M, Pumplin J and Yuan C P 2010 *Phys. Rev. D* **82**(7) 074024
[16] Aad G *et al.* 2014 *Journal of High Energy Physics* **2014**
[17] Pumplin J, Stump D R, Huston J, Lai H L, Nadolsky P and Tung W K 2002 *Journal of High Energy Physics* **2002** 012–012
[18] Aad G *et al.* (ATLAS Collaboration) 2011 *Phys. Rev. D* **83**(5) 052005
[19] Gleisberg T, Höche S, Krauss F, Schönherr M, Schumann S, Siegert F and Winter J 2009 *Journal of High Energy Physics* **2009** 007–007
[20] P N Rapheeha, X Ruan, G Mokgatitswane, S Dahbi and B Mellado 2021 *Background decomposition in $Z\gamma$ events used in the search for high-mass resonances* (to be published in the 2021 SAIP book of proceedings)
[21] Aad G *et al.* 2019 *Journal of Instrumentation* **14** P12006–P12006
[22] Aad G *et al.* (ATLAS Collaboration) 2020 Recommendations for the Modeling of Smooth Backgrounds Tech. rep. CERN Geneva